Thermal Excitation of Trivelpiece-Gould Modes in a Pure Electron Plasma

Francois Anderegg*, Nobuyasu Shiga*, James R. Danielson*, Daniel H.E. Dubin*, C. Fred Driscoll* and Roy W. Gould†

*Dept. of Physics and Institute for Pure and Applied Physical Sciences, UCSD, La Jolla CA USA 92093-0319
†California Institute of Technology, Mail Stop 128-95, Pasadena CA 91103

Abstract. Thermally excited plasma modes are observed in trapped, near-thermal-equilibrium pure electron plasmas over a temperature range of $0.05 < T < 5$ eV. The measured thermal emission spectra together with a separate measurement of the wave absorption coefficient uniquely determines the temperature. Alternately, kinetic theory including the antenna geometry and the measured mode damping (i.e. spectral width) gives the plasma impedance, obviating the reflection measurement. This non-destructive temperature diagnostic agrees well with standard diagnostics, and may be useful for expensive species such as anti-matter.

Even in a stable plasma there are a finite level of fluctuating electric field and plasma waves. The plasma waves are "normal modes" [1] of the system, and represent degrees of freedom which are excited in thermal equilibrium. Plasma waves are emitted by particles as they move about in the plasma, and they are absorbed (e.g. Landau-damped) by the plasma. The balance between emission and absorption leads to a thermal level of field fluctuation. Thermally excited modes can be a diagnostic tool for non-neutral plasmas as shown by Gould for cyclotron waves [2]. Similarly, center of mass modes are commonly used in the "single particle regime" with a highly tuned resonant circuit [3].

We describe measurements of spontaneous thermal excitation of Trivelpiece-Gould (TG) modes. The thermal radiation observed comes from collective plasma modes. The spectrum of these modes shows several well-separated peaks at the frequency of TG modes. The radiation we describe comes from one of these peaks, typically form the lowest longitudinal and radial mode number of an azimuthally symmetric mode.

Here, the spectrum of thermally-excited T-G modes is measured in near-thermal-equilibrium pure electron plasmas over a temperature range of $0.05 < kT < 5$ eV, using a room-temperature receiver. The received spectrum for each mode is nominally a Lorentzian at frequency f_0 with width γ, superimposed on a background noise level; non-Lorentzian spectra also occur, when the receiver noise and impedance is non-negligible. By Nyquist's theorem, these fluctuations represent thermal noise generated by the real part of the plasma impedance Z_p [4]. The area of the received spectral peak is proportional to kT, but it also depends on the antenna coupling as represented by Z_p. This impedance can be measured directly by a separate wave reflection/absorption measurement, or it can be calculated from a kinetic theory of random test particles. Overall, the technique allows a rapid non-destructive diagnostic of the plasma temperature with

CP606, *Non-Neutral Plasma Physics IV,* edited by F. Anderegg et al.

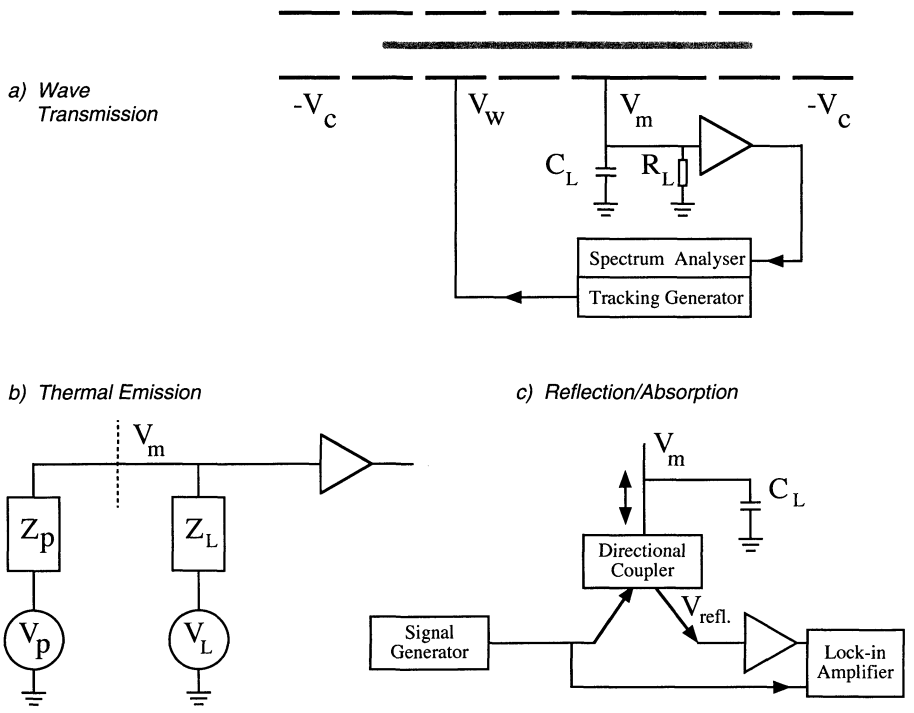

FIGURE 1. Schematic diagram of the cylindrical Penning-Malmberg trap with (a) the wave transmission/reception electronics; (b) the thermal emission equivalent circuit; and (c) the reflection/absorption electronics.

$\pm 25\%$ accuracy.

Fluctuation measurements were obtained from pure electron plasmas combined in two similar Penning-Malmberg traps, "EV" and "IV" [5], differing mainly in plasma diameter and magnetic field strength. The EV trap consists of a series of hollow conducting cylinders of radius $r_w = 3.8$ cm contained in ultra-high vacuum at $P \approx 10^{-10}$ Torr with a uniform axial magnetic field of $B = 375$ G. Electrons are injected from a hot tungsten filament, and contained axially by voltages $V_c \approx -200$ V on end electrodes. Typical plasmas have $N \approx 10^9$ electrons in a column length $L_p \approx 24$ cm, with a plasma radius $r_p \approx 1.7$ cm and a central density $n_0 \approx 10^7$ cm^{-3}. For IV, the parameters are $B = 30$ kG, $r_p = 0.2$ cm, $r_w = 2.86$ cm, and $L_p = 41$ cm.

The plasma density profile $n(r)$ and the thermal energy T are obtained by dumping the plasma axially and measuring the total charge passing through a hole in a scanning collimator plate. Both measurements require shot-to-shot reproducibility of the injected plasma, and we typically obtain variability $\delta n/n \leq 1\%$. The EV plasmas expand radially towards the wall with a characteristic "mobility" time of $\tau_m \approx 100$ sec, so the electrons are repetitively injected and dumped. On IV, a "rotating wall" perturbation at $f \sim$

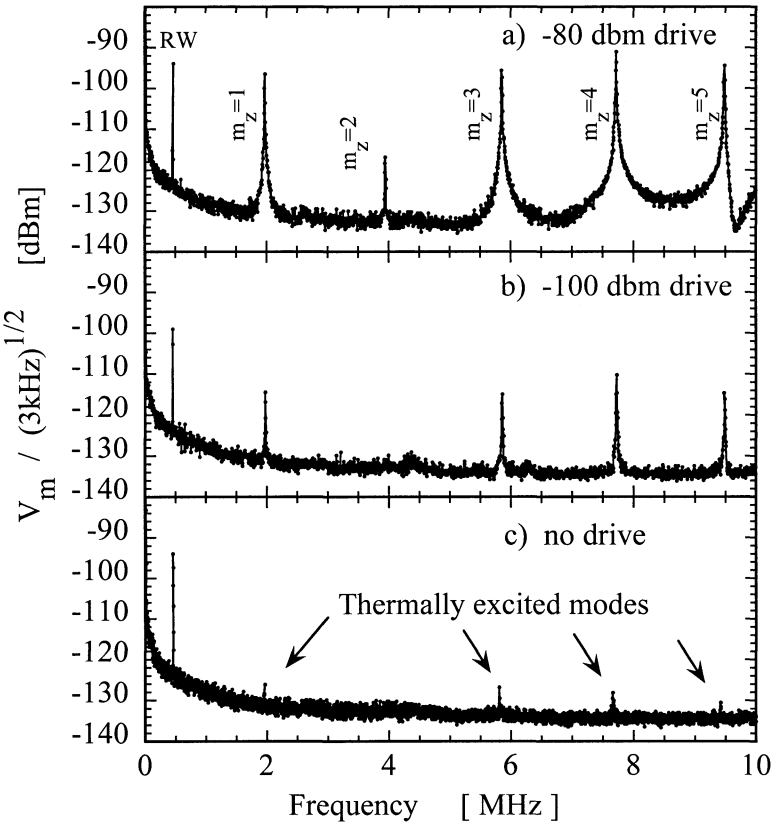

FIGURE 2. a) Spectrum of $m_\theta = 0$, $m_z = 1, 2,...5$ Trivelpiece-Gould modes for 3 drive amplitudes including no drive, i.e. thermally excited.

0.5 MHz is used to obtain steady-state confinement of the electron column [6].

The parallel temperature $T_\parallel$ of the electrons can be measured by slowly lowering the confinement voltage and measuring the escaping charge [7, 8]. On EV, the electrons equilibrate to $T \lesssim 1$ eV soon after injection, whereas the electrons in IV cool to $T \approx 0.05$ eV due to cyclotron radiation. To control the temperature, we apply auxilliary "wiggle" heating by modulating one electrode voltage at a frequency $f = 0.8 - 1.0$ MHz. The amplitude and duration of the heating is adjusted to obtain temperatures up to $T \lesssim 5$ eV; higher temperatures cause background gas ionization and a slow increase in N.

We perform plasma wave *transmission* experiments by applying an RF voltage of amplitude V_w to a (360°) wall electrode at one end of the column (Fig. 1a). V_w induces density perturbations δn in the column which in turn induce the measured voltages V_m on a (360°) receiving electrode with finite load impedance. The load impedance is

$R_L = 750\ \Omega$ (IV) or $50\ \Omega$ (EV) in parallel with $C_L \simeq 440$ pF (IV) and $C_L = 165$ pF (EV).

Figures 2a and 2b show the spectrum of standing $m_\theta = 0$ Trivelpiece-Gould modes [9] excited with excitations of $V_w = -80$ dbm (22 μV) and -100 dBm (2.2 μV) at frequencies $f = 0.01 - 10$ MHz. These standing waves are plasma oscillations with wavenumber $k_z = \pi m_z / L_p$. Here $\omega_p \equiv (2\pi)\ 28\ \text{MHz}\ (n/10^7\ \text{cm}^{-3})^{1/2}$ is the plasma frequency, modified by the finite trap radius, at frequencies

$$f \approx \frac{\omega_p}{2\pi} r_p m_z \frac{\pi}{L_p} \left[\frac{1}{2} \ln\, r_w/r_p\right]^{1/2} \left[1 + \frac{3}{2}\left(\frac{\bar{v}}{v_\phi}\right)^2\right]. \tag{1}$$

The axial mode number is $m_z = 1, 2 \ldots 5$, and thermal corrections depend on the ratio of $\bar{v} \equiv (kT/m)^{1/2}$ to the wave phase velocity v_ϕ. In this paper, we focus only on the lowest radial mode $m_r = 1$.

The peak amplitudes are proportional to V_w, as expected for a linear system; the lesser sensitivity for $m_z = 2$ is due to the placement z_c and length ($L_c = 11.7$ cm) of the detection cylinder. The peak amplitudes for the continuous sinusoidal modes are independent of the bandwidth (BW = 3 kHz) of the spectrum analyzer; whereas the spectral amplitude of the inter-mode noise decreases as $(\text{BW})^{-1/2}$ as expected. At $V_w = -100$ dBm, the mode fluctuations have amplitude $\delta n/n \sim 10^{-5}$. The peak labelled RW is the rotating wall drive; the measurements presented here have also been obtained with the drive off.

Small peaks representing thermally excited modes are still visible in Fig. 2c when the transmitter electrode is grounded ($V_w = 0$). These peaks have amplitudes of $-124\ \text{dBm}/\sqrt{3\text{kHz}}$, representing voltage fluctuations on the electrode with spectral intensity $V_m \approx 2.6nV/\sqrt{\text{Hz}}$.

Figure 3 shows received spectra of the thermally excited $m_z = 1$ mode for 4 similar plasmas of different temperature. The mode frequency f_0 increases with temperature, as expected from Eq. (1). The width of the spectral peak represents mode damping, and this width increases substantially as Landau damping becomes significant for $T \gtrsim 0.5$ eV. We will see below that the integral $\int \frac{V^2}{BW} df$ corrected for the load impedance will correspond to the thermal energy $\frac{1}{2}kT$.

Figure 1b shows a circuit modeling the reception of thermal noise from the plasma. The thermally excited fluctuating plasma voltage V_p flows through a plasma impedance Z_p, then through a load impedance Z_L with its inevitable noise V_L. Near a mode at frequency $\omega_0 = 2\pi f_0$, the plasma admittance Z_p^{-1} is given by a simple pole, as

$$Z_p^{-1} = \frac{R_p^{-1}\gamma_p}{i(\omega - \omega_0) + \gamma_p}. \tag{2}$$

As will be seen below, the plasma resistance R_p depends on γ_p and on the geometric coupling between the plasma and the receiving electrode. The measured load resistance R_L and capacitance C_L give

$$Z_L^{-1} \equiv R_L^{-1} + i\omega C_L \tag{3}$$

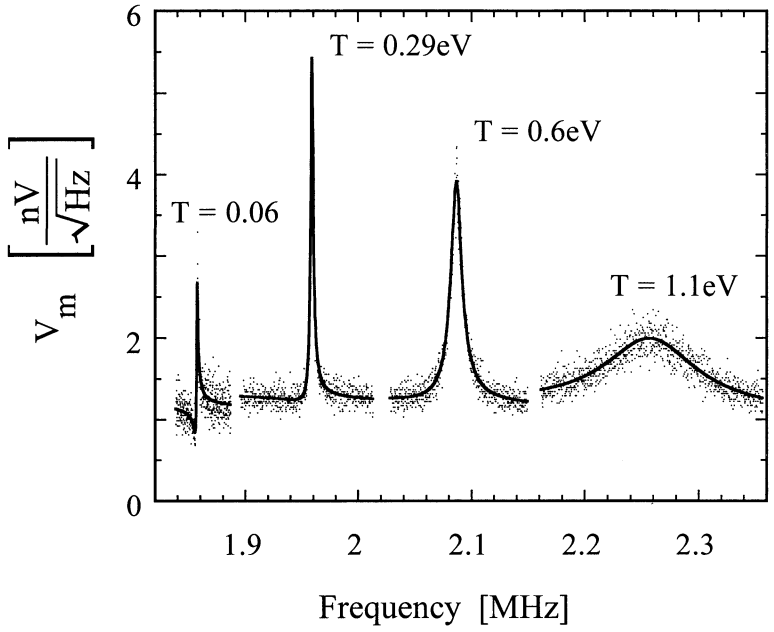

FIGURE 3. Spectra of the thermally excited $m_\theta = 0$, $m_z = 1$, mode for different plasma temperature; the solid lines are fits to Eq. (4).

which is essentially constant over the mode resonance; this simple Z_L differs from the resonant-circuit loads commonly used in harmonic traps with a small number of particles [3].

Nyquist's theorem says that the spectral density of the square of the noise voltage is proportional to the kT times real part of the impedance, for both the plasma and the load noise sources [4]. A voltage-divider fraction $Z_L/(Z_p + Z_L)$ of the plasma voltage V_p will be measured on the electrode as V_m, together with an analogous fraction of the (uncorrelated) load noise, giving

$$\frac{V_m^2(f)}{df} = 4kT\, Z_p^{\mathrm{Re}} \left(\frac{Z_L}{Z_p + Z_L}\right)^2 + 4kT_L\, Z_L^{\mathrm{Re}} \left(\frac{Z_p}{Z_p + Z_L}\right)^2, \tag{4}$$

where $Z^{\mathrm{Re}} \equiv \mathrm{Re}\{Z\}$ and $Z^{\mathrm{Im}} \equiv \mathrm{Im}\{Z\}$. Using Eqs. (2) and (3), Eq. (4) can be explicitly written as

$$\frac{V_m^2(f)}{df} = 4kT_L\, Z_L^{\mathrm{Re}} + 4\frac{kT}{R_p}|Z_L|^2 \left(1 + \frac{Z_L^{\mathrm{Re}}}{R_p}\right)^{-2} \left[\frac{\alpha\gamma_{\mathrm{tot}}^2 - \beta\gamma_{\mathrm{tot}}(\omega - \omega_0)}{\gamma_{\mathrm{tot}}^2 + (\omega - \omega_0')^2}\right], \tag{5}$$

where

$$\begin{aligned}
\gamma_{\text{tot}} &= \left(1+\frac{Z_L^{\text{Re}}}{R_p}\right)\gamma_p \\
\omega_0' &= \omega_0 - \frac{Z_L^{\text{Im}}}{R_p}\gamma_p \\
\alpha &= 1-\frac{T_L}{T}\left\{\frac{Z_L^{\text{Re}}}{R_p}-2\frac{(Z_L^{\text{Re}})^2}{|Z_L|^2}\right\} \\
\beta &= 2\frac{T_L}{T}\left(1+\frac{Z_L^{\text{Re}}}{R_p}\right)\frac{Z_L^{\text{Re}}Z_L^{\text{Im}}}{|Z_L|^2}.
\end{aligned}$$

For relatively high plasma temperature, one can assume $\beta = 0$, and Eq. (5) describes a simple Lorentzian resonance superimposed on a uniform noise background. The spectrum is then characterized by 4 parameters: 3 characterize the resonance, as frequency $\omega_0/2\pi$, width γ_{tot}, and amplitude kT/R_p; and the 4th parameter of the load temperature T_L sets the background level. Best-fit values of kT/R_p obtained for the 4 spectra of Fig. 3, together with the separately measured plasma temperature T, then imply values of $R_p = 81$, 160, 850 and 7800 Ω.

In contrast, both T and R_p are uniquely determined by the emission spectrum alone for regimes where the load-generated noise "filtered" by the plasma resonance becomes significant, as in the $T = 0.06$ eV case of Fig. 3. Here, the spectrum is not a simple Lorentzian, and a fifth parameter, R_p/Z_L^{Re}, is required for a complete fit to Eq. (5). The plasma impedance is effectively filtering the noise generated by Z_L^{Re} creating a "dip" in the trace at ω_0. The imaginary part of Z_L creates a small shift $\omega_0 - \omega_0'$ of the plasma peak relative to the noise "dip." For the narrow peak of $T = 0.06$ eV, the frequency shift is comparable to the width of the plasma mode. Under these conditions, the noise generated by Z_L^{Re} is effectively performing the reflection measurement described below. A 5-parameter fit to this spectrum gives $T = 0.03$ eV and $R_p = 81$ Ω, consistent with the 4-parameter fit and separately measured temperature.

For most of our data, we have near-Lorentzian V_m spectra; and to use them as a temperature diagnostic, R_p must be obtained independently. This plasma resistance R_p (and full impedance Z_p) can be obtained either from a reflection/absorption measurement, as shown in Fig. 1c; or from a first-principles kinetic analysis of the plasma fluctuations [1] including the trap/antenna geometry, as discussed below.

The direct reflection/absorption measurement of Z_p uses a directional coupler and lock-in detector to determine the reflection coefficient $\tilde{r}(f)$ for a weak wave at frequency f incident on the receiving antenna and plasma. This (complex) reflection coefficient is defined as the voltage fraction (and phase) which is reflected by the plasma-loaded antenna compared to that reflected by an open circuit without antenna or plasma, i.e.

$$\tilde{r} \equiv V_{\text{refl}}(\text{plasma})/V_{\text{refl}}(\text{open}). \tag{6}$$

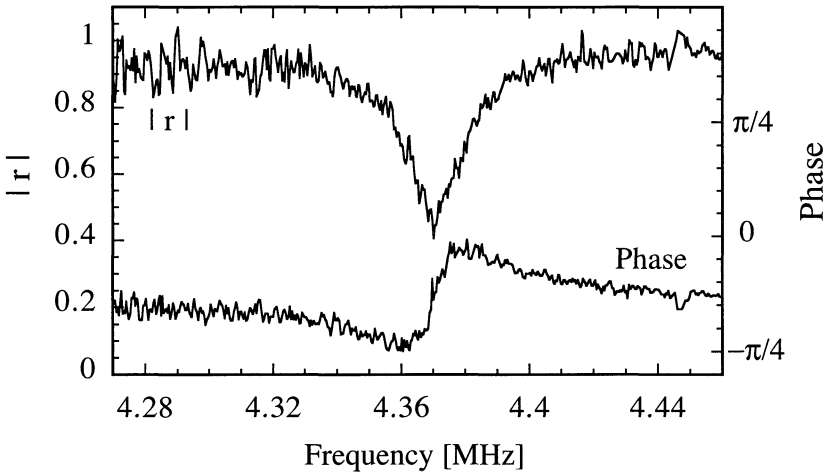

FIGURE 4. Measured magnitude and phase of the reflection coefficient $\tilde{r}$.

This reflection coefficient depends on the impedance $Z_{\rm tot}$ connected to the directional coupler compared to the impedance $Z_0 = 50\ \Omega$ of the coupler itself, as [4]

$$Z_{\rm tot} = Z_0 \frac{(1+\tilde{r})}{(1-\tilde{r})}. \tag{7}$$

Here, $Z_{\rm tot}^{-1} = Z_p^{-1} + i\omega C_L$ is the total impedance of the plasma-loaded antenna, given by the plasma impedance Z_p in parallel with the capacitance C_L of the electrode and connecting cable.

Figure 4 shows the measured amplitude and phase of the reflected wave as the frequency is scanned across the $m_z = 1$ mode. (The data is from EV, where the frequencies are about $2\times$ higher than on IV.) Away from the mode, the entire signal is reflected. On resonance, about 60% of the incident wave is absorbed by the plasma, and 40% is reflected. A fit to the data gives the parameters of $Z_{\rm tot}$ as $f_0 = 4.37$ MHz, $\gamma/\omega = 2.4\times10^{-3}$, $R_p = 153\ \Omega$, and $C_L = 155$ pF. In essence, the depth of the absorption dip indicates how close R_p is to the 50 Ω of the directional coupler.

Alternately, a kinetic analysis reproduces the Nyquist theorem and gives R_p in terms of geometry and the mode damping γ_p. Integrating in frequency over the $m_\theta = 0$, $m_z = 1$, $m_r = 1$ mode gives a mean-square radial electric field on the wall of

$$\delta E_r^2 = kT \frac{8}{r_w^2 L_p} \cos^2\!\left(\frac{\pi z}{L_p}\right) \mathcal{J}(x) \left(\frac{R_p}{R_p + Z_L^{\rm Re}}\right) \frac{1}{4\pi\varepsilon_0}, \tag{8}$$

with $\mathcal{J}(x) \equiv [J_0^2(x) + J_1^2(x)]/(\partial D/\partial x)^2$, $D(x) \equiv xJ_1(x)\ln(r_w/r_p) - J_0(x)$, and $x = (\omega_p^2/\omega_0^2 - 1)^{1/2}\pi r_p/L_p$. Here, J_0 and J_1 are Bessel functions of the first kind, and for simplicity we have kept only lowest-order terms in r_w/L_p. Note that δE_r represents the radial component of the electric field at the wall, not the total wave electric

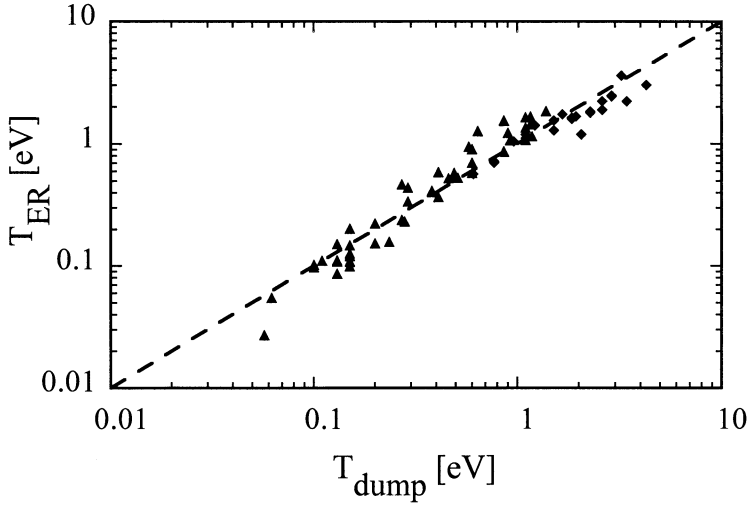

FIGURE 5. Plasma temperature measured by emission/reflection technique, compared to the standard dump temperature measurement. The triangles are from the IV apparatus and the diamonds are from the EV apparatus.

field. This δE_r induces the measured fluctuating charge δQ on a cylindrical electrode of length L_c located at z_c, given by

$$\delta Q^2 = 2kT \left(\frac{R_p}{R_p + Z_L^{\mathrm{Re}}}\right) \mathcal{G}\,(4\pi\varepsilon_0) \tag{9}$$

with

$$\mathcal{G} \equiv L_p \frac{\mathcal{J}(x)}{\pi^2} \left[\sin\left(\frac{\pi(z_c + L_c)}{L_p}\right) - \sin\left(\frac{\pi z_c}{L_p}\right)\right]^2.$$

From the circuit perspective of Fig. 1b, $\omega_0^2 \delta Q^2$ represents the mode-integrated mean-square current, so $\omega_0^2 \delta Q^2 = \int df (V_p^2/df)(Z_p + Z_L)^{-2} = 2kT\,\gamma_p/(R_p + Z_L^{\mathrm{Re}})$ using Eqs. (2) and (3). Thus, we obtain

$$\gamma_{\mathrm{tot}} \equiv \gamma_p + \gamma_L = (R_p + Z_L^{\mathrm{Re}})\,\omega_0^2\,\mathcal{G}\,(4\pi\varepsilon_0). \tag{10}$$

That is, the kinetic analysis gives mode-integrated fluctuating currents proportional to kT, and identifies the total mode damping as proportional to the sum of the resistances R_p and Z_L^{Re} in the plasma and the load, scaled by the geometric factors $\mathcal{G}$ and ω_0.

For typical EV parameters of $r_p = 1.66$ cm, $r_w = 3.8$ cm, $L_p = 23.5$ cm, $z_c = 0$, $L_c = 5.8$ cm, $n = 8.45 \times 10^6$ cm^{-3}, and $\omega_p^2/\omega_0^2 = 41.3$, we obtain $x = 1.41$, $D = 0.072$, $\mathcal{G} = 1$ cm/2.02 and $\gamma_{\mathrm{tot}}/\omega_0 = (R_p + Z_L^{\mathrm{Re}})/7.2 \times 10^4 \Omega$.

It is important to note that Z_L^{Re} contributes to the mode damping on an equal footing with R_p. For example, an external load resistance of $Z_L^{\mathrm{Re}} = 72\ \Omega$ induces a baseline

mode damping of $\gamma_L/\omega_0 = 10^{-3}$. Thus, even small receiver resistance can contribute significantly to mode damping.

Figure 5 displays the inferred plasma temperature T_{ER}, obtained from the emission spectra and reflection/absorption measurements, versus the plasma temperature T_{dump} measured by dumping the plasma. The plasma temperature was controlled by adding "wiggle heating" at one end of the column, and data was taken for plasmas with a range of "geometric" parameters (n, r_p, L_p) on both EV (diamond symbols) and IV (triangle symbols). The values of T_{ER} were obtained from 4-parameter fits to the emission spectra, together with a separately obtained value of R_p.

Conceptually, determining R_p amounts to determining the plasma/antenna geometry factor $\mathcal{G}$ of Eq. (10). Moreover, $\mathcal{G}$ does not depend significantly on plasma temperature, so one determination of $\mathcal{G}$ suffices for all plasmas with the same geometric parameters.

On EV, we measured R_p from the reflection/absorption technique over a plasma temperature range of $0.5 < T < 5eV$. This gave $30 < R_p < 2000\Omega$, implying "internal" plasma dampings of $5 \times 10^{-4} < \gamma_p/\omega_0 < 0.02$. Over this temperature range, we verified that the observed γ_{tot} is proportional to the total resistance, with a best-fit value giving $\mathcal{G} = 1$ cm/2.26. This is in close agreement with the algebraic formula for $\mathcal{G}$.

On IV, the value of R_p was determined from a single 5-parameter fit to the non-Lorentzian "$T = 0.06$" spectrum of Fig. 3, giving $\mathcal{G} = 1$ cm/5.3. A direct calculation of $\mathcal{G}$ using the "measured" $r_p = 0.2$ cm gives $\mathcal{G} = 1$ cm/3.45; but this discrepancy is within the uncertainty in the determination of small plasma radius r_p on IV.

It should be emphasized that steady-state plasmas often exhibit spectral peaks which are 10 to 100 times larger than thermal, because the mode is being externally driven. For example, noise on the ostensibly steady confinement voltages V_c or ambient RF signals may stimulate particular plasma modes without proportionately increasing the plasma temperature. Similarly, particular modes in a warm plasma can be damped (i.e. cooled) with an external feedback circuit, decreasing the peak mode amplitude by 25×, without substantially cooling the plasma. That is, the plasma modes are relatively weakly coupled to the theorist's thermal bath [10]. Since each mode has only kT of energy compared to the 10^9 kT in the entire plasma, it is rather easy for particular experimental manipulations to overwhelm the mode energy; so this thermometer is rather fragile.

ACKNOWLEDGMENTS

This work is supported by Office of Naval Research Grant No. N00014-96-1-0239 and National Science Foundation Grant PHY-9876999. We thank Dr. R.E. Pollock for suggesting this work and demonstrating that thermally excited TG modes can be observed; and Dr. T.M. O'Neil for many fruitful discussions.

REFERENCES

1. N. Krall and A.W. Trivelpiece, *Principles of Plasma Physics* (McGraw-Hill, 1973), Ch. 11.
2. R.W. Gould, Phys. Plasmas **2**, 2151 (1995).
3. D.J. Wineland and H.G. Dehmelt, J. Appl. Phys. **46**, 919 (1975).

4. R.W. Gould, "Thermal Excitation of Modes in a Non-Neutral Plasma," in this proceedings.
5. F. Anderegg, X.-P. Huang, E. Sarid, and C.F. Driscoll, Rev. Sci. Instrum. **68**, 2367 (1997).
6. F. Anderegg, E.M. Hollmann, and C.F. Driscoll, Phys. Rev. Lett. **81**, 4875 (1998); E.M. Hollmann, F. Anderegg, and C.F. Driscoll, Phys. Plasmas **7**, 2776 (2000).
7. D.L. Eggleston, C.F. Driscoll, B.R. Beck, A.W. Hyatt, and J.H. Malmberg, Phys. Fluids B **4**, 2432 (1992).
8. B.R. Beck, J. Fajans, and J.H. Malmberg, Phys. Plasmas **3**, 1250 (1996).
9. S.A. Prasad and T.M. O'Neil, Phys. Fluids **26**, 665 (1983); A.W. Trivelpiece and R.W. Gould, J. Appl. Phys. **30**, 1784 (1959).
10. C.F. Driscoll, J.H. Malmberg and K.S. Fine, Phys. Rev. Lett. **60**, 1290 (1988); T.M. O'Neil and D.H.E. Dubin, Phys. Plasmas **5**, 2163 (1998).